Journal of The Electrochemical Society, **153** (3) G229-G233 (2006)
0013-4651/2006/153(3)/G229/5/$20.00 © The Electrochemical Society

Shallow Junction Ion Implantation in Ge and Associated Defect Control

A. Satta, E. Simoen,*,z T. Janssens, T. Clarysse, B. De Jaeger, A. Benedetti, I. Hoflijk, B. Brijs, M. Meuris, and W. Vandervorst

IMEC, B-3001 Leuven, Belgium

We have studied implant-induced damage, defect annealing, and recrystallization of B, Ga, P, As, and Sb introduced in Ge by ion implantation at high doses, such that dopant chemical concentrations are above the corresponding solubility in Ge, with energies that target about 100-nm junction depths. It is shown that the amount of damage induced in the Ge lattice increases with the mass of the implanted ion, as expected. Implanted B produces local amorphous regions, although crystalline Ge zones are present in the implanted layer. P is a self-amorphizing ion, creating a continuous amorphous layer during implantation. However, a low thermal budget is sufficient to fully regrow the amorphous layer, without evidence of residual extended defects, as evaluated by cross-sectional transmission electron microscopy. Conversely, high concentrations of As cause a significant decrease of the regrowth rate of the damaged layer during rapid thermal annealing in the 400–600°C range studied. Finally, high-dose implantation of heavy ions such as Sb induces dramatic morphologic changes in Ge that are not recovered by post-implant rapid thermal annealing.
© 2006 The Electrochemical Society. [DOI: 10.1149/1.2162469] All rights reserved.

Manuscript submitted June 24, 2005; revised manuscript received November 30, 2005. Available electronically January 24, 2006.

Ion implantation of dopant elements into Ge is relevant for the application of doped Ge layers in high-mobility nanometer-scaled devices,[1] in nuclear-radiation detectors,[2] and in photodetectors for the communications wavelength regime (1.3–1.55 μm).[3] Moreover, the fact that the behavior of commonly implanted doping elements from groups III and V is significantly different in Ge compared to Si draws the attention to critical issues of junction formation by ion implantation, such as crystal damage extension, defect recovery, and recrystallization temperatures and rates in Ge. Extensive comparisons have been made in the past regarding the damage creation in Si, Ge, and SiGe alloys by Si ion implantation.[4-6] It has been clearly established that for the same implantation conditions, significantly more damage is created in Ge than in Si.[4-7] This is in part related to the higher stopping power of germanium atoms (heavier mass), resulting in a higher energy density per atom in the collision cascades produced by the bombarding ions.[5] A second factor contributing to a higher retained lattice disorder is the reduced mobility of the defects in the collision cascades.[5]

In contrast to the behavior for Si, the recovery of implant-induced lattice disorder starts in Ge at significantly low temperatures. Annealing of localized damage occurs in the temperature range of 150–400°C, depending on the implant dose and species.[7-9] It has been shown that for 60-keV 1×10^{15} atom/cm^2 B implantations, the associated damage is removed by a single annealing stage at 150°C,[9] which is explained by a high rate of defect annealing already during the implant. However, annealing up to 450°C can be necessary for the removal of acceptor-like defects induced in Ge by heavier mass ion implantations.[7] Similar to the Si case, the regrowth of amorphous Ge is initiated at the amorphous–crystalline interface, controlled by the formation and motion of vacancies.[10] The reordering of amorphous layers requires typically higher annealing temperatures than the ones necessary to cure localized damaged regions,[8] although it may occur with reasonable rate at 300–400°C, depending on crystal orientation, implanted doses, and dopant species.[8,10,11]

This paper summarizes our recent studies on the damage induced into the Ge lattice by the implantation of dopant elements with different mass, such as B, Ga, P, As, and Sb, traditionally used to form p^+n and n^+p junctions in both Si and Ge semiconductors.[12,13] The maximum equilibrium solid solubilities of these elements in Ge, according to Trumbore,[14] are reported in Table I. In our experiments, the implantations are carried out with high ion doses that give rise to a dopant chemical concentration above these solubility values. The goal is the formation of low-resistivity and shallow (100 nm, indicatively) junctions, which could serve as highly doped drain regions in a Ge metal oxide semiconductor (MOS) transistor. In Table I we report the sheet resistance values of Ge junctions, as calculated from the chemical profiles of the studied dopants (with corresponding junction depths X_j), assuming the activation levels given by the maximum solubility for each element. From these calculations it emerges that Ga as acceptor and P as donor element are the most promising candidates for shallow junction formation in Ge. We show that the measured junction sheet resistance deviates significantly from the calculated values and is usually higher (Table I). The problems related to such high-dose implantations, such as crystal damage, defect recovery, amorphization, and regrowth, and formation of precipitates and their possible impact on the electrical activity of the implanted dopant, are discussed for the different doping elements.

An additional constraint in the formation of such shallow junctions comes from the annealing technique. In order to be compatible with deep submicrometer complementary metal-oxide semiconductor (CMOS) processing only a limited thermal budget is allowed, relying on rapid thermal annealing (RTA). This should minimize dopant diffusion in order to reach the targeted X_j.

Experimental

Czochralski-grown 100-mm-diam Ge wafers, 500-μm-thick, ⟨100⟩-oriented, Sb-doped and Ga-doped with resistivities of about 23 and 11 Ω-cm, respectively, were obtained from Umicore. A 10-nm plasma-enhanced chemical vapor deposited (PECVD) SiO_2 layer was deposited prior to ion implantation onto the Ge crystals. Implantations with several doping elements, from B to heavier elements, such as, in order, P, Ga, As, and Sb, were performed at Ion-Beam Services (IBS France) using a 7° tilt to avoid channeling effects. The dopant doses vary from 1 to 5×10^{15} atom/cm^2, targeting chemical concentrations above equilibrium solid solubility. The dopant energies were chosen according to the element mass in order to achieve the objective of about a 100-nm junction depth. The annealing of the samples was performed in N_2 atmosphere in the Heatpulse 610 RTP system at annealing temperatures not higher than 600°C and times not longer than 60 s. The chemical profile of the dopants was studied by secondary ion mass spectrometry (SIMS), while the variable probe spacing (VPS) technique[15] was used to characterize the sheet resistance of the Ge junctions in order to ensure low probe penetration into the Ge crystal and avoid probing of the substrate.[16] Transmission electron microscopy (TEM), scanning electron microscopy (SEM), and Rutherford backscattering spectroscopy (RBS) were used to investigate the implant-induced

* Electronical Society Active Member.
z E-mail: eddy.simoen@imec.be

Table I. Maximum solid solubilities for the common doping elements in Ge[14] and calculated sheet resistance corresponding with the junction depth X_j of column 5. This is compared with the measured sheet resistance after a 600°C 1-s rapid thermal anneal.

Dopant element	Equilibrium solid solubility (atom/cm^3)[a]	Expected *Rs* (Ω/□)	Measured *Rs* (Ω/sq)	X_j (nm)	SiO_2 cap layer
B	5.5×10^{18}	315	200	140	10 nm
Ga	4.9×10^{20}	34	84	115	10 nm
P	2.0×10^{20}	42	75	92	None
As	8.1×10^{19}	79	257	120	10 nm
Sb	1.2×10^{19}	163 (Box profile)	-	100	-

[a] Trumbore[14]

damage and Ge amorphization in the as-implanted samples and the residual crystalline defects and the Ge recrystallization after sample annealing.

Results and Discussion

In the next two paragraphs, the crystal disorder induced by ion implantation of a light acceptor element such as B is compared to a heavier p-type element such as Ga and the damage created by heavier mass donor elements such as P, As, and Sb is illustrated and discussed. However, it becomes clear that the damage recovery is not solely determined by the ion mass but also depends on the implanted species involved (chemical effect).

Acceptor elements: B (and Ga).— The chemical profile of B introduced in crystalline Ge (c-Ge) with an energy of 6 keV to a dose of 3×10^{15} atom/cm^2 through a 10-nm SiO_2 cap layer is shown in Fig. 1. As-implanted and annealed (at 400°C for 60 s) profiles completely overlap due to the low diffusivity of B in Ge at low temperature (<800–900°C).[17] The peak of the chemical profile is located at about 10 nm from the SiO_2/Ge interface with a B maximum concentration of 8×10^{20} atom/cm^3. This high concentration level gives rise most likely to boron precipitates or clustering in the c-Ge already during implantation. Cross-sectional TEM images of as-implanted samples (Fig. 2a) show the presence of dark contrast regions (indicated by white arrows in the pictures) located at the B concentration peak. After annealing at 400°C for 60 s, the dark features remain in the same position, indicating that the applied thermal budget is not sufficient to dissolve these structures (Fig. 2b). The TEM images additionally show that extended damage is created by the implantation, with amorphous regions alternating with crystalline Ge zones (Fig. 2a). Upon annealing at 400°C, the amorphous zones are regrown into crystalline Ge, although some residual crystal disorder seems to remain (Fig. 2b). The sheet resistance *Rs* of these B junctions is however about 200 Ω/□, (Fig. 3), lower than that expected from the B solubility in Ge (Table I). Gusev et al.[18] also reported an above-solubility activation for high-dose B implants, suggesting an activity enhancement due to the extensive implant damage (possible amorphization) in the Ge crystal. Moreover,

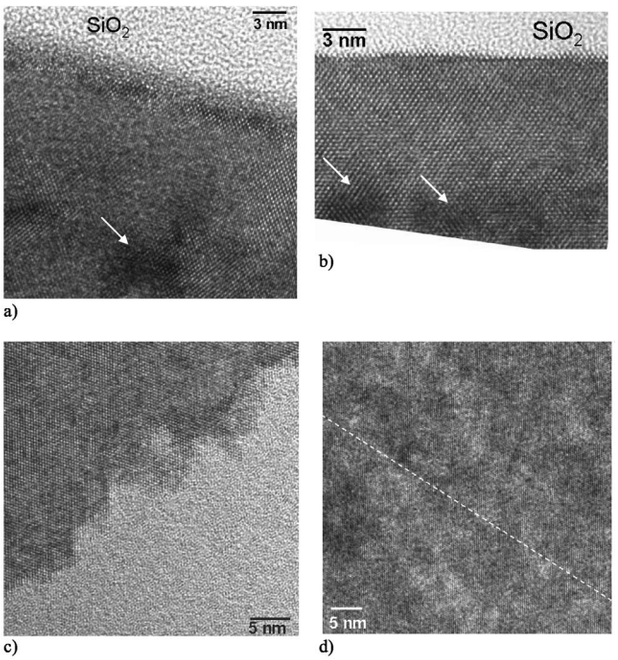

Figure 2. Cross-sectional TEM micrographs of 6-keV 3×10^{15} atom/cm^2 boron-implanted crystalline Ge, as-implanted (a); after annealing at 400°C, 60 s (b); the α/c interface of the preamorphized Ge, as-implanted with B (c); and the original α/c interface after annealing at 400°C for 60 s (d). The dashed line in (d) indicates the original location of the α/c interface.

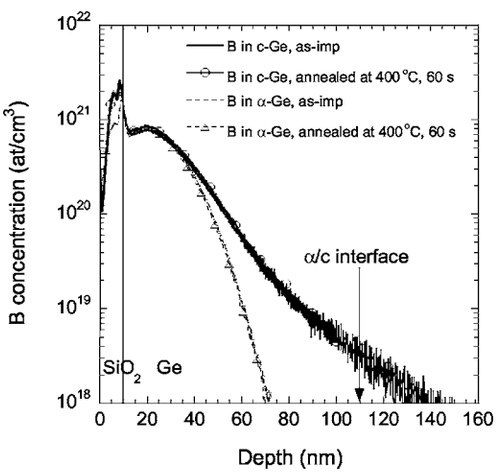

Figure 1. Chemical profiles of 6-keV 3×10^{15} atom/cm^2 boron, as-implanted and annealed at 400°C in c-Ge and in Ge preamorphized by a Ge implant of 100 keV energy to a dose of 1×10^{15} atom/cm^2. The α/c interface is located at a 100 nm depth into Ge.

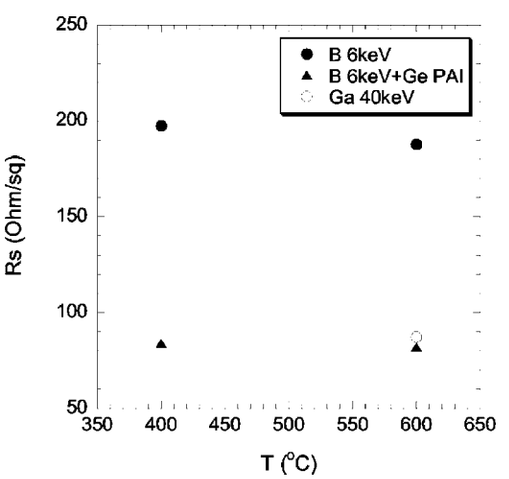

Figure 3. Sheet resistance of B, B + Ge preamorphization, and Ga-doped Ge junctions annealed at 400 and 600°C for 60 s. The dose of B and Ga species was 3×10^{15} atom/cm^2. The error of each measurement point is about 1%, which is within the plot symbol size.

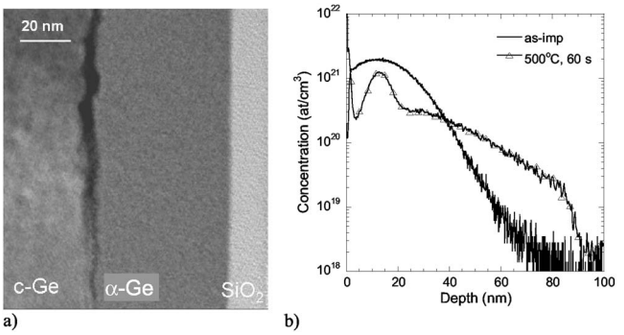

Figure 4. TEM cross-sectional micrograph of Ge crystal, as-implanted with P 25 keV 3×10^{15} atom/cm^2 (a). As-implanted and annealed (at 500°C for 60 s) profiles of P implanted with 15 keV to a dose of 5×10^{15} atom/cm^2 (b).

the R_s does not decrease upon higher thermal budgets (up to 600°C, 60 s), suggesting that the B clusters are stable and their bonding is not easily broken.[19] This is further supported by the comparison with the sheet resistance of a 3×10^{15} atom/cm^2 40-keV Ga implantation, annealed at 600°C for 60 s (Fig. 3). The Ga junction depth is about 120 nm at 1×10^{18} atom/cm^3 (from SIMS profiles, not shown here), while the sheet resistance value of 85 Ω/□ suggests a higher activation level compared to the B case. Differently from B, Ga is self-amorphizing at the considered dose and energy, while a full recrystallization occurs after annealing. This strongly suggests the use of a Ge preamorphization implant to improve the activation level of B in Ge.

We have performed a Ge preamorphization by a Ge implant of 100-keV 1×10^{15} atom/cm^2, which gives rise to a 100-nm continuous amorphous layer (α-Ge) (as shown by TEM analysis), prior to the same B implantation performed in the c-Ge substrate.[19] The B profile is now entirely located in the amorphous Ge region. Figure 1 shows that the Ge preamorphization suppresses the large B channeling and leads to the formation of a shallower and more abrupt junction. The sheet resistance of this B junction formed from the amorphous Ge phase (Fig. 3) indicates a significantly enhanced activation level of B in Ge with respect to the B junction formed from crystalline Ge.

The amorphous/crystalline Ge interface produced by the Ge amorphizing implant is very rough (Fig. 2c). The pronounced interface roughness is possibly enhanced by a regrowth into c-Ge occurring already during implantation. Applying a low thermal budget (400°C, 60 s) is sufficient to fully recrystallize the amorphous layer up to the surface, in agreement with past studies reporting enhancement of the Ge regrowth rate by high levels of B doping.[11]

Remarkably, no extended defects were found at the original amorphous/crystalline interface (Fig. 2d) and in the regrown layer by means of cross-sectional TEM analysis, meaning a defect density lower than 10^7/cm^2. Moreover, although the B concentration peak in the α-Ge is at the same level as that in the c-Ge, B precipitation or clustering has not been observed by TEM,[19] both in the amorphous phase just after implantation and following the regrowth into c-Ge. This indicates that the B solubility achieved under solid-phase epitaxial regrowth conditions is much higher than that of B in c-Ge.

Donors, heavier-mass doping elements: P, As, and Sb.— A doping element such as P, almost three times heavier than B, is expected to produce much more extensive damage in the Ge matrix. Past studies[7] have indicated 1×10^{14} atom/cm^2 as the limit dose for P self-amorphization, when an energy of 15 keV is employed. A P implant of 3×10^{15} atom/cm^2 with the energy of 25 keV (through a 10-nm SiO_2 layer) creates by itself a continuous amorphous layer of approximately 60-nm depth (Fig. 4a), while the junction depth of such implant is 90 nm (as indicated by SIMS analysis). This

Table II. Sheet resistance and activation percentage for a 15 keV for 5×10^{15} atom/cm^2 P implant, after rapid thermal annealing at 500 and 600°C for 1 s. The error on the *Rs* values is 1%, while the error on the activation percentage is determined mainly by the assumption on the mobility values in Ge.

RTA	Junction depth (nm)	R_s (Ω/□)
500°C, 60 s	92	117
600°C, 1 s	92	75

P-implanted amorphous layer is fully recrystallized after annealing at 400°C for 60 s,[20] similar to the B-doped amorphous Ge layer. Also in this case, moreover, the TEM analysis did not reveal the presence of residual extended crystal disorder.

However, although P is self-amorphizing at high doses and therefore a high P solubility may be expected, similar as for the B case, P clustering may still occur. The chemical profile of P, implanted with 15-keV energy to a 5×10^{15} atom/cm^2 dose and annealed at 500°C, shows a peculiar peak located in the region where P atoms reside with the highest concentration after implantation (Fig. 4b). From the comparison of the as-implanted and annealed SIMS profiles, it is clear that mobile P atoms diffuse rapidly both toward the surface and into the bulk, according to the concentration-enhanced diffusivity of P in Ge at high concentrations ($>2 \times 10^{19}$ atom/cm^3).[20-22] However, the P atoms located in the region of the concentration peak (10–15 nm from the surface) are only slightly mobile, indicating a possible presence of P clusters.

The relatively high sheet resistance value measured for this P junction at 500°C (Table II) indicates the presence of inactive P, possibly in clusters. Differently from the B precipitates discussed in the previous session, the P features appearing in the SIMS profile are very unstable as a higher thermal budget enables them to be easily dissolved.[22] The concentration peak located at 10–15 nm (Fig. 4b) disappears upon annealing at higher temperature, 600°C,[22] while simultaneously the sheet resistance decreases significantly, without being accompanied by a junction deepening (Table I). The sheet resistance of 75 Ω/□ obtained at 600°C for a 92-nm junction depth (reported in Tables I and II) corresponds to a P active concentration of $5–6 \times 10^{19}$ atom/cm^3, which is the maximum active level we have also measured for deep P junctions in Ge.[20] This active level is clearly below the maximum solid solubility reported in the literature for P in Ge.

The chemical profile of As implanted in Ge with 50-keV energy and 3×10^{15} atom/cm^2 dose through 10-nm SiO_2 (Fig. 5a) is characterized by a junction depth of 80 nm at 1×10^{18} atom/cm^3. TEM investigation reveals that such implant creates an amorphous

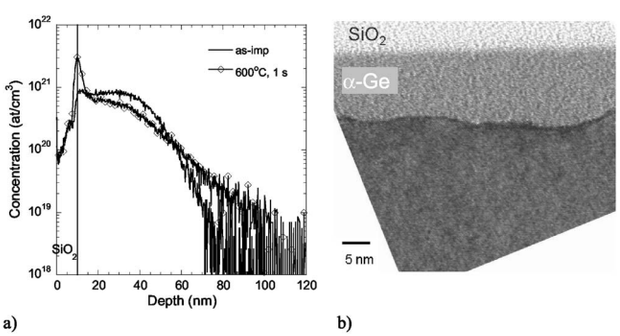

Figure 5. As-implanted chemical profile of As implanted with 50 keV energy and 3×10^{15} atom/cm^2 dose (a). The α/c interface is located at 50 nm from the SiO_2/Ge interface, as indicated by TEM analysis. Cross sectional TEM image of the same As-doped Ge layer after annealing at 400°C for 60 s (b).

Table III. Sheet resistance of 50-keV 3×10^{15} atom/cm^2 As-doped Ge junctions, annealed at 400°C for 60 s and at 500°C for 1 and 60 s.

Anneal	R_s ($\Omega/\square$)
400°C, 60 s	1680
500°C, 1 s	901
500°C, 60 s	257

depth of 50 nm into the Ge. Therefore, the flat concentration peak of 8×10^{20} atom/cm^3 in the as-implanted profile, extending approximately from 10 to 40 nm, is totally enclosed in the amorphous region (Fig. 5a). In contrast with the behavior of the B and P-doped amorphous Ge layers previously discussed, the As-doped amorphous Ge is not fully regrown upon the limited thermal budget of 400°C, 60 s. A residual amorphous layer of 10–15 nm (the thickness range is due to pronounced interface roughness) remains after annealing, indicating retardation in the regrowth of As-doped Ge (Fig. 5b). The presence of a residual amorphous region may explain the high R_s values of the As junctions annealed at 400°C, 60 s and 500°C, 1 s, as reported in Table III, whereby the longer anneal at 500°C corresponds to a narrower residual amorphous zone.

Suni et al.[11] have reported a reduction of the regrowth rate of Ge highly doped with As. Concentrations above 1×10^{20} atom/cm^3 induce a significant drop in the recrystallization velocity with respect to the case of lower As concentrations. As the solubility of implanted dopants may constrain the regrowth of highly doped Ge, it has been speculated that precipitation of impurities can be the cause of retardation of the regrowth.[11] A doping level above 1×10^{20} atom/cm^3 is indeed higher than the reported solubility of As in Ge (Table I) and the formation of As precipitates, stable at high temperatures,[23] and associated punched-out dislocation loops has been reported in the literature.[24] As shown above, in the case of P, the inactive fraction is in a less stable form that can be more easily dissolved, which could explain the different recrystallization rate of high-dose P and As implantations in germanium. For B, the high regrowth rate has been related to the charge state or Fermi-level effect on the formation rate of vacancies at the amorphous/crystalline interface.[11] This follows, among others, from the fact that the regrowth rate increases with increasing B concentration.[11]

Annealing with a higher thermal budget (600°C, 1 s), at which a full recrystallization of the damaged Ge layer is expected, causes As atoms to move into the bulk and toward the surface, with visible segregation at the SiO_2/Ge interface (Fig. 5a). The As-diffused profiles are not box-shaped, which turn out to be an exclusive characteristic of P. However similar to P, high in-diffusion and out-diffusion rates are observed.

When much heavier ions are introduced in Ge by ion implantation at high doses, a severe and irreversible damage, consisting of surface cratering, can be produced. This has been observed in the past for heavy elements, such as In, Bi, and Sn, implanted in Ge at high doses.[25] Similarly, we have seen that the introduction of Sb in Ge is accompanied by dramatic damage consisting of unusual void formation. After implantation, large craters extending for tens of nanometers deep beneath the surface are revealed by X-SEM (Fig. 6a). The depth of the craters is dependent on the Sb implant dose.[26] This peculiar implantation damage produced by high-dose implants has been attributed more recently to formation of voids in the early stage of implantation, followed by an effective clustering of vacancies beneath the surface at room temperature, with consequent void growth in the direction perpendicular to the surface.[27] We have seen that the extensive damage remains after annealing, as shown by RBS measurements in the channeling mode (Fig. 6b) with the persistent presence of craters at the Ge surface. This seriously restricts the usefulness of Sb (or, in general, of heavy-mass elements, such as In) for shallow junction formation in Ge by ion implantation.

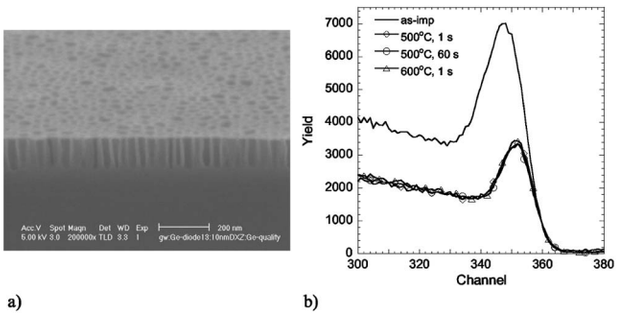

Figure 6. X-SEM image of Ge implanted with 70 keV 10^{15} atom/cm^2 Sb (a). RBS spectra of Ge layers, doped with 70 keV 3×10^{15} atom/cm^3 Sb, after implantation and after annealing at different temperatures and times. The RBS spectrum of crystalline Ge is reported as a reference (b).

Conclusions

The damage induced in the Ge lattice during high-dose implantation of B, Ga, P, As, and Sb doping elements depends strongly on the corresponding atom mass. A small, light atom such as B produces restricted amorphous regions that are regrown during annealing at low temperature (400°C), although some residual lattice disorder seems to remain. Importantly, B concentrations as high as $\sim 10^{21}$ atom/cm^3 lead to precipitation or clustering during implantation, which does not dissolve by postimplant anneals up to 600°C. Only by a junction formation with Ge preamorphization followed by solid-phase epitaxial regrowth of the B-doped Ge does the B solubility in Ge increase considerably, giving rise to a significantly higher amount of substitutionally active B atoms, without residual defects in the regrown layer.

For the doses considered in this study, P is a self-amorphizing element with a continuous amorphous layer formed during implantation. Full regrowth occurs by applying a small thermal budget, with no evidence of remaining damage. High P concentrations ($>10^{21}$ atom/cm^3) may give rise, however, to the formation of inactive, unstable P clusters.

A serious regrowth retardation of highly As-doped Ge possibly indicates a solid solubility limit for As atoms to be incorporated at high concentrations in the Ge lattice. Higher thermal budgets are needed to fully regrow the damaged doped layer into crystalline Ge.

The remarkable radiation-induced damage produced by the heaviest element considered in this study, Sb, clearly limits the usefulness of Sb implantation for shallow junction formation in Ge. The dramatic peculiar damage created by this heavy dopant is not recovered by post-implant rapid thermal anneals.

IMEC assisted in meeting the publication costs of this article.

References

1. H. Shang, H. Okorn-Schmidt, K. K. Chan, M. Copel, J. A. Ott, P. M. Kozlowski, S. E. Steen, S. A. Cordes, H. -S. P. Wong, E. C. Jones, and W. E. Haensch, *Tech. Dig. - Int. Electron Devices Meet.*, **2002**, 441.
2. R. E. Jones, S. G. Thomas, S. Bharatan, R. Thoma, C. Jasper, T. Zirkle, N. V. Edwards, R. Liu, X. D. Wang, Q. Xie, C. Rosenblad, J. Ramm, G. Isella, H. von Känel, J. Oh, and J. C. Campbell, *Tech. Dig. - Int. Electron Devices Meet.*, **2002**, 793.
3. Y. S. Suh, M. S. Carroll, R. A. Levy, M. A. Sahiner, G. Bisognin, and C. A. King, *IEEE Trans. Electron Devices*, **52**, 91 (2005).
4. T. E. Haynes and O. W. Holland, *Appl. Phys. Lett.*, **61**, 61 (1992).
5. D. Y. C. Lie, A. Vantomme, F. Eisen, T. Vreeland, Jr., M.-A. Nicolet, T. K. Carns, V. Arbet-Engels, and K. L. Wang, *J. Appl. Phys.*, **74**, 6039 (1993).
6. D. Y. C. Lie, *J. Electron. Mater.*, **27**, 377 (1998).
7. K. Benourhazi and J. P. Ponpon, *Nucl. Instrum. Methods Phys. Res. B*, **71**, 406 (1992).
8. J. W. Mayer, L. Eriksson, S. T. Picraux, and J. A. Davies, *Can. J. Phys.*, **46**, 663 (1968).
9. P. J. McDonald and D. W. Palmer, *Inst. Phys. Conf. Ser.*, No. 23, **7**, 504 (1975).
10. L. Csepregi, R. P. Küllen, and J. W. Mayer, *Solid State Commun.*, **21**, 1019 (1977).
11. I. Suni, G. Goltz, M.-A. Nicolet, and S. S. Lau, *Thin Solid Films*, **93**, 171 (1982).
12. A. Satta, E. Simoen, M. Meuris, T. Janssens, T. Clarysse, C. Demeurisse, I. Hoflijk, and W. Vandervorst, in *Proceedings of the International Symposium on Advanced*

Gate Stack, Source/Drain, and Channel Engineering for Si-Based CMOS: New Materials, Processes, and Equipment, E. Gusev, L.-J. Chen, H. Iwai, D.-L. Kwong, M. C. Öztürk, F. Roozeboom, and P. J. Timans, Editors, PV 2005-05, pp. 468–474, The Electrochemical Society Proceedings Series, Pennington, NJ (2005).
13. A. Satta, E. Simoen, T. Janssens, A. Benedetti, T. Clarysse, B. De Jaeger, L. Geenen, B. Brijs, M. Meuris, and W. Vandervorst, in *Crystalline Defects and Contamination: Their Impact and Control in Device Manufacturing IV - DECON IV*, B. O. Kolbesen, C. L. Claeys, L. Fabry, and F. Tardif, Editors, PV 2005-10, pp. 52–58, The Electrochemical Society Proceedings Series, Pennington, NJ (2005).
14. F. A. Trumbore, *Bell Syst. Tech. J.*, **39**, 205 (1960).
15. T. Clarysse, D. Vanhaeren, I. Hoflijk, and W. Vandervorst, *Mater. Sci. Eng., R.*, **47**, 123 (2004).
16. T. Clarysse, P. Eyben, T. Janssens, I. Hoflijk, D. Vanhaeren, A. Satta, M. Meuris, W. Vandervorst, J. Bogdanowicz, and G. Raskin, *J. Vac. Sci. Technol. B*, In press.
17. S. Uppal, A. F. W. Willoughby, J. M. Bonar, N. E. B. Cowern, T. Grasby, R. J. H. Morris, and M. G. Dowsett, *J. Appl. Phys.*, **96**, 1376 (2004).
18. V. M. Gusev, M. I. Guseva, E. S. Ionova, A. N. Mansurova, and C. V. Starinin, *Phys. Status Solidi A*, **21**, 413 (1974).
19. A. Satta, E. Simoen, T. Clarysse, T. Janssens, A. Benedetti, B. De Jaeger, M. Meuris, and W. Vandervorst, *Appl. Phys. Lett.*, **18**, 172109 (2005).
20. A. Satta, T. Janssens, T. Clarysse, E. Simoen, M. Meuris, A. Benedetti, I. Hoflijk, B. De Jaeger, C. Demeurisse, and W. Vandervorst, *J. Vac. Sci. Technol. B*, In press.
21. S. Matsumoto and T. Niimi, *J. Electrochem. Soc.*, **125**, 1307 (1978).
22. A. Satta, T. Janssens, T. Clarysse, E. Simoen, A. Benedetti, L. Geenen, M. Meuris, and W. Vandervorst, In preparation.
23. G. H. Schwuttke and J. K. Howard, *J. Appl. Phys.*, **39**, 1581 (1968).
24. Yu. P. Kabanov, L. M. Morgulis, and Yu. A. Osip'yan, *Sov. Phys. Solid State*, **10**, 523 (1968).
25. O. W. Holland, B. R. Appleton, and J. Narajan, *J. Appl. Phys.*, **54**, 2295 (1983).
26. T. Janssens, C. Huyghebaert, D. Vanhaeren, G. Winderickx, A. Satta, M. Meuris, and W. Vandervorst, *J. Vac. Sci. Technol. B*, In press.
27. N. Nitta, M. Taniwaki, Y. Hayashi and T. Yoshiie, *J. Appl. Phys.*, **92**, 1799 (2002)